FINITE ELEMENT MODEL FOR FORMING PROCESS OF THERMOPLASTIC COMPOSITE SHELLS

M. T. Abadi (abadi@ari.ac.ir)
Aerospace Research Institute
Ministry of Science, Research and Technology, Tehran, Iran

Keywords: *forming, thermoplastic composite, woven fabric, unidirectional fiber*

Abstract

A continuum-based shell finite element method is presented to model the forming process of thermoplastic plies reinforced with unidirectional fibers or woven fabric. At forming temperature, the composite ply is considered as an incompressible viscous shell reinforced with inextensible fibers. Using Mindlin-Reissner theory and updating ply thickness, the intra-ply shear and transverse flow mechanisms are regarded in the forming process analysis. To eliminate the accumulation of computational errors in each increment, the kinematical constrains are defined according to the reference configuration. Using an appropriate solution method and eliminating quasi-static assumptions considered in the previous research works, the calculated deformed shell geometry satisfies the governing equations according to the current material properties at the end of each increment.

1 Introduction

Sheet forming is an effective fabrication method to deform thermoplastic composite laminates into the final shape. To successfully investigate the formability of composite laminates and optimize the forming process parameters, an accurate and effective model with appropriate computational method is essential. The results of forming analysis are also used to estimate the mechanical behavior of final deformed geometry. Finite element analysis is an appropriate technique to model the forming process of complex geometries.

Forming of thermoplastic composite laminates starts with heating to the temperature that the resin melts and the fibers find enough flexibility to match the die geometry. The heated laminates are subsequently formed by a mechanical contact or hydrostatic pressure. Since the formed laminates are cooled while the load is applied, the solidified resin highly prevents to recover the deformation after load removal. Experiments have shown that continuous fibers define inextensible orientations in the reinforced thermoplastic laminates during forming process [1]. Due to high ratio of bulk to shear viscosity, thermoplastic reinforced sheets behave like an incompressible material at forming temperature [2]. The Kinematical constrains and anisotropic behaviour cause special considerations must be taken into account in the numerical analysis.

A continuum approach is commonly used to model the behavior of pre-heated thermoplastic laminates reinforced with continuous fibers so that the composite ply is considered as an anisotropic continuum material with single or two preferred material directions for unidirectional and woven fibers reinforcement, respectively. Spencer [3] formulated a constitutive equation for flow of reinforced composite materials which having viscous response at forming temperature. Ó Brádaigh and Pipes [4] proposed a mixed finite element formulation to analyze forming process of the composite sheet reinforced with single continuous fiber using a continuum model. This approach was applied to simulate the plane stress and plane strain laminate deformation problems [5-6]. Johnson and Pickett [7] developed an explicit finite element method using shell theory with plane stress assumption to analyze the thermoplastic composite deformation.

In the previous finite element formulations, the forming process was assumed to be accomplished in quasi-static conditions in which the laminate velocity field was computed at the start of increment. Then, the new nodal coordinates were obtained by assuming a constant velocity during each increment. Furthermore, constant fiber directions and laminate thickness were assumed in

each increment. The assumption of a constant velocity and invariant geometric characteristics may make considerable computational errors [6, 8]. In this case, the kinematical constrains are not satisfied and subsequently inaccurate large stress is obtained at the end of time increment.

In some recent research works [9-10], the woven fabric thermoplastic laminates were modelled using a non-orthogonal constitutive equation in which the viscous behaviour of melted resin was ignored at forming temperature. Experimental studies [11-12] showed that the deformation force and defects on the finished parts highly depend on the rate of deformation. Therefore, a rate dependent model is required to analyze the viscous flow of thermoplastic laminates at forming temperature.

In the present research work, a continuum-based shell finite element method is presented to model the forming process of thermoplastic plies reinforced with unidirectional fibers or woven fabric. At forming temperature, the composite ply is considered as an incompressible viscous shell reinforced with inextensible fibers. Using Mindlin-Reissner theory and updating ply thickness, the intra-ply shear and transverse flow mechanisms are regarded in the forming process analysis. A penalty method is used to enforce the kinematical constrains to the finite element formulation. To eliminate the accumulation of computational errors in each increment, the kinematical constrains are defined according to the reference configuration. Using an appropriate solution method and eliminating quasi-static assumptions considered in previous research works, the calculated deformed shell geometry satisfies the governing equations according to current material properties at the end of each increment. The hemispherical forming process is analyzed using the present method and the results are evaluated in the regions that the woven fabric reinforced plies have high potential to wrinkle.

2 Kinematics

Consider a flat reinforced ply with a uniform thickness as a reference configuration and it is deformed to a curvilinear geometry as the forming process proceeds. A fixed rectangular coordinate system with unit vector $\mathbf{e}_i$ is considered so that the 1-2 plane coincides with the mid-plane at reference geometry. A typical point of reinforced ply has a position vector $\mathbf{X}$ (components X_k) in the reference configuration. The point moves to a position vector $\mathbf{x}_{(\mathbf{X},t)}$ (components x_i) with the velocity vector $\mathbf{v}_{(\mathbf{x},t)}$ (components v_i) in the deformed configuration at time t. Consider a unit vector normal to the mid-plane in the reference configuration. The unit vector rotates in the deformed geometry and the current direction is described by a unit vector $\mathbf{p}$ (components p_i). Due to Mindlin-Reissner theory, the unit vector may differ from the normal direction to the mid-surface in the deformed geometry. The motion of reinforced ply is described by

$$x_{i(X_k,t)} = \bar{x}_{i(X_\alpha,t)} + \frac{X_3}{H} h_{(X_\alpha,t)} p_{i(X_\alpha,t)} \qquad (1)$$

where $\bar{x}_i$ are the position vector components of corresponding point on mid-surface, 2H and $2h$ are the initial and current ply thickness, respectively. Throughout this paper, the Greek letters are used for indices in the range {1, 2}. Taking time derivative of Eq. (1) yields the velocity field as follows

$$v_i = \bar{v}_i + \frac{X_3}{H}\left(\dot{h}p_i + h\dot{p}_i\right) \qquad (2)$$

where $\bar{v}_i$ are the velocity vector components of corresponding point on mid-surface. In continuum-based shell theory, the momentum balance is not enforced for the relative motion in the direction of $\mathbf{p}$. Hence, the rate of thickness change is ignored in the calculation of velocity field and the ply thickness will be updated using the conservation of matter. The velocity of a point located in ply thickness is expressed in terms of the velocity of corresponding point in mid-surface and rate of rotation of vector $\mathbf{p}$, designated by $\mathbf{w}$ (components w_i). Thus, Eq. (2) can be written as

$$v_i = \bar{v}_i + \varepsilon_{ijk} \frac{h}{H} X_3 w_j p_k \qquad (3)$$

The macroscopic state of deformation is typically described using the deformation gradient tensor, designated by $\mathbf{F}$. Using Eq. (1), the components of the deformation gradient tensor are given by

$$F_{i\alpha} = \frac{\partial \bar{x}_i}{\partial X_\alpha} + \frac{X_3}{H}\frac{\partial(hp_i)}{\partial X_\alpha}, \quad F_{i3} = \frac{h}{H} p_i \qquad (4)$$

Since the reinforced ply is deformed as an incompressible material in forming process [2], the

determinant of deformation gradient tensor must be a unit value, i.e.

$$J = \det \mathbf{F} = 1. \tag{5}$$

At the mid-surface, the incompressibility constrain yields the current ply thickness as

$$\frac{1}{h} = \frac{1}{H} \det \begin{bmatrix} \frac{\partial \bar{x}_1}{\partial X_1} & \frac{\partial \bar{x}_1}{\partial X_2} & p_1 \\ \frac{\partial \bar{x}_2}{\partial X_1} & \frac{\partial \bar{x}_2}{\partial X_2} & p_2 \\ \frac{\partial \bar{x}_3}{\partial X_1} & \frac{\partial \bar{x}_3}{\partial X_2} & p_3 \end{bmatrix} \tag{6}$$

In the reference configuration, the unit vectors $\mathbf{A}^{(\lambda)}$ (components $A_i^{(\lambda)}$) are attributed along the tangent to the fiber directions (λ={1,2} for a ply reinforced with woven fibers and λ={1} for unidirectional fiber reinforcement) as shown in Fig. (1). At the reference configuration, all reinforcing fibers lie in planes parallel to mid-plane ($A_3^{(\lambda)}$=0). The fibers are regarded as material lines [3], in which the deformation gradient describes the transformation between the initial and deformed fiber directions as

$$a_i^{(\lambda)} = F_{i\alpha} A_\alpha^{(\lambda)} \tag{7}$$

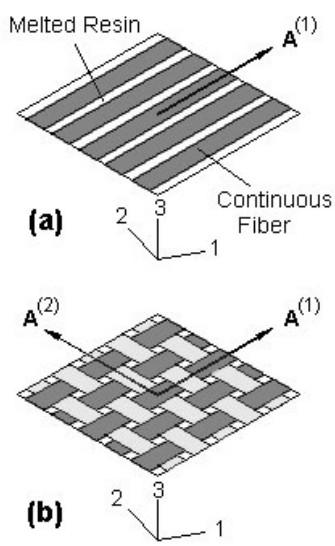

Fig. 1. a) A ply reinforced with unidirectional fibers b) A ply reinforced with woven fabric

where $a_i^{(\lambda)}$ are the components of vector along the tangent to the fiber directions in the deformed configuration and the repeated indices without parentheses imply summing over the range of the index. Since the continuous fibers define inextensible directions in the reinforced thermoplastic materials at the forming temperature [1], the vectors along fiber directions in the deformed geometry must be unit vectors, so

$$\begin{aligned} & a_r^{(\lambda)} a_r^{(\lambda)} - 1 = F_{r\alpha} F_{r\beta} A_\alpha^{(\lambda)} A_\beta^{(\lambda)} - 1 = \\ & 2\varepsilon_{\alpha\beta} A_\alpha^{(\lambda)} A_\beta^{(\lambda)} = 0 \end{aligned} \tag{8}$$

where $\varepsilon_{\alpha\beta}$ are the components of Green strain tensor. In order to enforce the inextensibility kinematical constrain to the weak form of momentum equation, a potential function is defined by

$$I = \frac{1}{2} \int_{\Omega_0} \alpha \sum_{\lambda=1}^{2} \left(\varepsilon_{\alpha\beta} A_\alpha^{(\lambda)} A_\beta^{(\lambda)} \right)^2 d\Omega_0, \quad \alpha_1 > 0 \tag{9}$$

where α is the penalty number, Ω_0 is the reference material volume. The potential function will be minimized when the kinematical constrain is satisfied. Since this is the only extremizing condition of the potential function, the variational calculus states the necessary condition to enforce the kinematical constrain as follows

$$\delta I = \int_{\Omega_0} \alpha \sum_{\lambda=1}^{2} \begin{bmatrix} \left(\varepsilon_{\alpha\beta} A_\alpha^{(\lambda)} A_\beta^{(\lambda)} \right) \times \\ A_\delta^{(\alpha)} A_\nu^{(\alpha)} \delta\varepsilon_{\delta\nu} \end{bmatrix} d\Omega_0 = 0. \tag{10}$$

3 Material Model

During forming at the temperature above the melting point of the thermoplastic materials, the continuous fiber-reinforced composite materials have been successfully modeled as an incompressible viscous or viscoelastic fluid constrained by inextensible fibers [3]. Due to the kinematical constrains in the reinforced materials, the reaction stress is considered including an arbitrary pressure and arbitrary tensions in the fiber directions. Hence, the stress has the form

$$\sigma_{ij} = -p\delta_{ij} + T^{(\lambda)} a_i^{(\lambda)} a_j^{(\lambda)} + \tau_{ij} \tag{11}$$

where σ_{ij} are the components of Cauchy stress tensor, p is an arbitrary pressure, $T^{(\lambda)}$ are arbitrary

tensions in the directions of $\mathbf{a}^{(\lambda)}$ and τ_{ij} are the components the extra-stress tensor which require a constitutive equation. The reaction stress does no work. Spencer [3] developed a constitutive equation for the linear viscous fluid reinforced with continuous fibers as follows

$$\tau_{ij} = 2\eta_0 D_{ij} + \sum_{\lambda=1}^{2}\sum_{\gamma=1}^{2} 2\eta_{\lambda\gamma}\left(a_i^{(\lambda)} a_k^{(\gamma)} D_{kj} + D_{ik} a_k^{(\gamma)} a_j^{(\lambda)}\right) \quad (12)$$

where η_0 and $\eta_{\lambda\gamma}$ are the material viscosities and D_{ij} are the components of rate-of-deformation tensor.

In the continuum-based shell theory, the stress normal to the mid-surface is set to zero. A corotational coordinate system with base vector $\hat{\boldsymbol{e}}_i$ is constructed at each point so that the plane defined by $\hat{\boldsymbol{e}}_1$ and $\hat{\boldsymbol{e}}_2$ is tangent to the mid-surface at that point. Since the normal stress is zero, the stress tensor in the corotational coordinate system can be written as

$$\hat{\sigma}_{ij} = T^{(\lambda)} \hat{a}_i^{(\lambda)} \hat{a}_j^{(\lambda)} + 2\eta_0\left(\hat{D}_{ij} + \hat{D}_{\alpha\alpha}\delta_{ij}\right) + 2\sum_{\lambda=1}^{2}\sum_{\gamma=1}^{2} \eta_{\lambda\gamma}\left(\hat{a}_i^{(\lambda)} \hat{a}_k^{(\gamma)} \hat{D}_{kj} + \hat{D}_{ik} \hat{a}_k^{(\gamma)} \hat{a}_j^{(\lambda)}\right) \quad (13)$$

The components of unit vector in fiber directions and rate-of-deformation tensor can be transformed to the co-rotational coordinate system as follows

$$\hat{a}_i = R_{ki} a_k \quad (14a)$$

$$\hat{D}_{ij} = R_{ki} R_{lj} D_{kl} \quad (14b)$$

where R_{ki} are the components of transformation matrix given by

$$R_{ki} = \hat{\mathbf{e}}_i \cdot \mathbf{e}_k \quad (15)$$

The extra-stress tensor can be obtained in the fixed coordinate system using the transformation in Eq. (13), i.e.

$$\tau_{ij} = 2\eta_0\left(D_{ij} + R_{p\alpha} R_{q\alpha} D_{pq} \delta_{ij}\right) + 2\sum_{\lambda=1}^{2}\sum_{\gamma=1}^{2} \eta_{\lambda\gamma}\left(a_i^{(\lambda)} a_k^{(\gamma)} D_{kj} + D_{ik} a_k^{(\gamma)} a_j^{(\lambda)}\right) \quad (16)$$

The Eq. (16) defined the extra-stress when the normal stress in corotational coordinate system is zero.

4 Finite Element Formulation

4.1 Finite Element Approximation of Motion

A continuum-based shell finite element model is presented to analyze large deformation of thermoplastic ply reinforced with continuous fibers. In the implementation of continuum-based theory, an underlying three-dimensional element is defined using the nodes of shell element and initial normal direction to the mid-plane. The motion of continuum element is then constrained to reflect the Mindlin-Reissner assumptions. For a given node I on the mid-plane at the reference configuration, two nodes of I^+ and I^- are defined on the initial normal located at the top and bottom surfaces of ply, respectively. Since the initial normal is described by two nodes in the top and bottom surfaces, the initial normal remains straight in the deformed geometry that reflects Mindlin-Reissner assumptions.

To derive finite element formulation, the mid-surface geometry is subdivided into a suitable number of shell elements. The components of nodal velocity and angular velocity vectors at the mid-surface are denoted by $v_{iI(t)}$ and $w_{iI(t)}$, in which lower and upper case subscripts are used for components and nodal numbers, respectively. Using Eq. (3), the velocity of ply in the continuum element is given by

$$v_{kI^+} = v_{kI} + h\varepsilon_{kil} w_{iI} p_l \quad (17a)$$

$$v_{kI^-} = v_{kI} - h\varepsilon_{kil} w_{iI} p_l \quad (17b)$$

For shape functions N_I considered in the shell element, the shape functions of continuum element in the top and bottom surfaces, designated by N_I^+ and N_I^-, respectively, become

$$N_{I^+(\xi,\eta,\zeta)} = \frac{1}{2} N_{I(\xi,\eta)}\left(1+\zeta\right) \quad -1 \le \zeta \le 1 \quad (18a)$$

$$N_{I^-(\xi,\eta,\zeta)} = \frac{1}{2} N_{I(\xi,\eta)}\left(1-\zeta\right) \quad -1 \le \zeta \le 1 \quad (18b)$$

Then, the velocity in continuum element can be written as

$$v_{k(\xi,\eta,\zeta)} = N_{I(\xi,\eta)} \delta_{ki} v_{iI} + \zeta \Lambda^I_{ki(\xi,\eta)} w_{iI} \quad (19)$$

where Λ^I_{ki} at node I are defined by

$$\Lambda^{I}_{ki(\xi,\eta)} = h_I \varepsilon_{kil} p_{Il} N_{I(\xi,\eta)} \quad (no\ sum\ on\ I) \tag{20}$$

For a given increment, the displacement in the continuum element can be approximated by Eq. (19), i.e.

$$u_{k(\xi,\eta,\zeta)} \approx N_{I(\xi,\eta)} \delta_{ki} u_{iI} + \zeta \Lambda^{I}_{ki(\xi,\eta)} \theta_{iI} \tag{21}$$

4.2 Principle of Virtual Work

The weak form of momentum equation, the traction boundary conditions and the interior traction continuity conditions are defined by the principle of virtual work. The virtual mid-surface nodal displacement and transverse plane rotation, designated by δu_{iI} and $\delta\theta_{iI}$, respectively, define virtual displacement field in the continuum element. The weak form is obtained by taking the product of the momentum equation with the virtual displacement and integrating over the element volume, which gives

$$\delta u_{iI}\left(f^{\text{int}}_{iI} - f^{ext}_{iI}\right) + \delta\theta_{iI}\left(m^{\text{int}}_{iI} - m^{ext}_{iI}\right) = 0. \tag{22}$$

where f^{int}_{iI}, f^{ext}_{iI}, m^{int}_{iI} and m^{ext}_{iI} denote, respectively, the components of internal and external forces and moments applied at node I defined by

$$f^{\text{int}}_{iI} = \int_{\Omega^e_0} \frac{\partial N_I}{\partial X_p} J F^{-1}_{pk} \tau_{ki} d\Omega_0 \tag{23a}$$

$$f^{ext}_{iI} = \int_{\Omega^e_0} N_I \rho_0 b_i d\Omega_0 + \int_{\Gamma^0_\sigma} N_I s^0_i d\Gamma_0 \tag{23b}$$

$$m^{\text{int}}_{iI} = \int_{\Omega^e_0} \zeta \frac{\partial \Lambda^I_{qi}}{\partial X_p} J F^{-1}_{pk} \tau_{kq} d\Omega_0 \tag{23c}$$

$$m^{ext}_{iI} = \int_{\Omega^e_0} \zeta \Lambda^I_{ki} \rho_0 b_k d\Omega_0 + \int_{\Gamma^0_\sigma} \zeta \Lambda^I_{ki} s^0_k d\Gamma \tag{23d}$$

Where s^0_i are the components of traction forces applied on the reference exterior surfaces denoted by Γ^0_σ, ρ_0 is initial material density and b_i are the components of body forces. Since inertia force has negligible effects in the typical forming process, it was eliminated in the linear momentum equation. Using Shape functions in Eq. (10) yields the inextensibility constrain for nodal displacement vector

$$\begin{aligned} \delta I = \delta u_{iI} \int_{\Omega_0} \alpha \sum_{\lambda=1}^{2} \begin{bmatrix} \left(\varepsilon_{\alpha\beta} A^{(\lambda)}_\alpha A^{(\lambda)}_\beta\right) \times \\ A^{(\lambda)}_\delta A^{(\lambda)}_\nu \dfrac{\partial \varepsilon_{\delta\nu}}{\partial u_{iI}} \end{bmatrix} d\Omega_0 + \\ \partial\theta_{iI} \int_{\Omega_0} \alpha \sum_{\lambda=1}^{2} \begin{bmatrix} \left(\varepsilon_{\alpha\beta} A^{(\lambda)}_\alpha A^{(\lambda)}_\beta\right) \times \\ A^{(\lambda)}_\delta A^{(\lambda)}_\nu \dfrac{\partial \varepsilon_{\delta\nu}}{\partial \theta_{iI}} \end{bmatrix} d\Omega_0 = 0 \end{aligned} \tag{24}$$

In order to enforce the inextensibility kinematical constrain to the solution of Eq. (22), the weak form of momentum equation must be modified by combining it with Eq. (24) as follows

$$\begin{aligned} &\delta u_{iI}\left(f^{\text{int}}_{iI} - f^{ext}_{iI} + f^{con}_{iI}\right) + \\ &\delta\theta_{iI}\left(m^{\text{int}}_{iI} - m^{ext}_{iI} + m^{con}_{iI}\right) = 0. \end{aligned} \tag{25}$$

where f^{con}_{iI} and m^{con}_{iI} are the kinematical nodal force and moment, respectively, defined by

$$f^{con}_{iI} = \int_{\Omega_0} \alpha \sum_{\lambda=1}^{2} \begin{bmatrix} \left(\varepsilon_{\alpha\beta} A^{(\lambda)}_\alpha A^{(\lambda)}_\beta\right) \times \\ A^{(\lambda)}_\delta A^{(\lambda)}_\nu \dfrac{\partial N_I}{\partial X_\delta} F_{i\nu} \end{bmatrix} d\Omega_0 \tag{26a}$$

$$m^{con}_{iI} = \int_{\Omega_0} \alpha \sum_{\lambda=1}^{2} \begin{bmatrix} \zeta\left(\varepsilon_{\alpha\beta} A^{(\lambda)}_\alpha A^{(\lambda)}_\beta\right) \times \\ A^{(\lambda)}_\delta A^{(\lambda)}_\nu \dfrac{\partial \Lambda^I_{pi}}{\partial X_\delta} F_{p\nu} \end{bmatrix} d\Omega_0 \tag{26b}$$

In Eq. (25), the terms in parentheses must be vanished for any arbitrary virtual nodal displacement and rotation values, i.e.

$$f^{res}_{iI} = f^{\text{int}}_{iI} - f^{ext}_{iI} + f^{con}_{iI} = 0. \tag{27a}$$

$$m^{res}_{iI} = m^{\text{int}}_{iI} - m^{ext}_{iI} + m^{con}_{iI} = 0. \tag{27b}$$

where f^{res}_{iI} and m^{res}_{iI} are the components of the residual force and moment applied at node I, respectively. The solution of above equations yields the deformed geometry regarding to the inextensibility constrain. The finite element formulation depends nonlinearly to the nodal displacement and rotation vectors because the stress tensor and fiber directions are nonlinear function of the current material geometry. In the present work, a Newton-Raphson method is used to calculate the

deformed geometry. Considering Taylor expansion of Eq. (27) and dropping terms of higher order than linear displacement and rotation increments result in

$$\left(K_{ijIJ}^{fu}\Big|^{\text{int}} - K_{ijIJ}^{fu}\Big|^{ext} + K_{ijIJ}^{fu}\Big|^{con}\right)\Delta u_{jJ} + \left(K_{ijIJ}^{f\theta}\Big|^{\text{int}} - K_{ijIJ}^{f\theta}\Big|^{ext} + K_{ijIJ}^{f\theta}\Big|^{con}\right)\Delta\theta_{jJ} = -f_{iI}^{res} \tag{28a}$$

$$\left(K_{ijIJ}^{mu}\Big|^{\text{int}} - K_{ijIJ}^{mu}\Big|^{ext} + K_{ijIJ}^{mu}\Big|^{con}\right)\Delta u_{jJ} + \left(K_{ijIJ}^{m\theta}\Big|^{\text{int}} - K_{ijIJ}^{m\theta}\Big|^{ext} + K_{ijIJ}^{m\theta}\Big|^{con}\right)\Delta\theta_{jJ} = -m_{iI}^{res} \tag{28b}$$

where $K_{ijIJ}^{fu}\Big|^{\cdots}$, $K_{ijIJ}^{f\theta}\Big|^{\cdots}$, $K_{ijIJ}^{mu}\Big|^{\cdots}$ and $K_{ijIJ}^{m\theta}\Big|^{\cdots}$ are the components of external, internal and kinematical Jacobean matrices defined by

$$K_{ijIJ}^{fu}\Big|^{\cdots} = \frac{\partial f_{iI}^{\cdots}}{\partial u_{jJ}}, \quad K_{ijIJ}^{f\theta}\Big|^{\cdots} = \frac{\partial f_{iI}^{\cdots}}{\partial \theta_{jJ}}$$
$$K_{ijIJ}^{mu}\Big|^{\cdots} = \frac{\partial m_{iI}^{\cdots}}{\partial u_{jJ}}, \quad K_{ijIJ}^{m\theta}\Big|^{\cdots} = \frac{\partial m_{iI}^{\cdots}}{\partial \theta_{jJ}} \tag{29}$$

The external force and moment Jacobean matrices are defined for the follower loads and moments that their values and directions depend on the configuration of the body. Taking the displacement derivative of internal force defined in Eq. (23) yields the internal Jacobean matrix

$$K_{ijIJ}^{fu}\Big|^{\text{int}} = \int_{\Omega_0^e} \frac{\partial N_I}{\partial X_p}\begin{pmatrix} \dfrac{\partial J}{\partial u_{jJ}} F_{pk}^{-1}\tau_{ki} + \\ J\dfrac{\partial F_{pk}^{-1}}{\partial u_{jJ}}\tau_{ki} + \\ JF_{pk}^{-1}\dfrac{\partial \tau_{ki}}{\partial u_{jJ}} \end{pmatrix} d\Omega_0 \tag{30}$$
$$= \int_{\Omega^e}\left[\begin{pmatrix} \dfrac{\partial N_I}{\partial x_k}\dfrac{\partial N_J}{\partial x_j} - \dfrac{\partial N_I}{\partial x_j}\dfrac{\partial N_J}{\partial x_k} \end{pmatrix}\tau_{ki} + \dfrac{\partial N_I}{\partial x_k}\dfrac{\partial \tau_{ki}}{\partial u_{jJ}}\right] d\Omega$$

The nodal displacement derivative of extra-stress tensor can be written as [8]

$$\frac{\partial \tau_{ki}}{\partial u_{jJ}} = \eta_0\begin{bmatrix} \dfrac{\partial N_J}{\partial x_i}\left(\dfrac{1}{\Delta t}\delta_{kj} - \dfrac{\partial v_k}{\partial x_j}\right) + \\ \dfrac{\partial N_J}{\partial x_k}\left(\dfrac{1}{\Delta t}\delta_{ij} - \dfrac{\partial v_i}{\partial x_j}\right) + \end{bmatrix} +$$
$$\eta_0 R_{p\alpha}R_{q\alpha}\begin{bmatrix} \dfrac{\partial N_J}{\partial x_q}\left(\dfrac{1}{\Delta t}\delta_{pj} - \dfrac{\partial v_p}{\partial x_j}\right) + \\ \dfrac{\partial N_J}{\partial x_p}\left(\dfrac{1}{\Delta t}\delta_{qj} - \dfrac{\partial v_q}{\partial x_j}\right) \end{bmatrix}\delta_{ki} +$$
$$\sum_{\lambda=1}^{2}\sum_{\gamma=1}^{2}\eta_{\lambda\gamma}\begin{bmatrix} a_k^{(\lambda)}a_p^{(\gamma)}\dfrac{\partial N_J}{\partial x_i}\left(\dfrac{1}{\Delta t}\delta_{pj} - \dfrac{\partial v_p}{\partial x_j}\right) + \\ a_k^{(\lambda)}a_p^{(\gamma)}\dfrac{\partial N_J}{\partial x_p}\left(\dfrac{1}{\Delta t}\delta_{ij} - \dfrac{\partial v_i}{\partial x_j}\right) + \\ 2\dfrac{\partial N_J}{\partial x_q}\begin{pmatrix} \delta_{kj}a_q^{(\lambda)}a_p^{(\gamma)}D_{pi} + \\ \delta_{pj}a_k^{(\lambda)}a_q^{(\gamma)}D_{pi} + \\ \delta_{pj}a_q^{(\gamma)}a_i^{(\lambda)}D_{kp} + \\ \delta_{ij}a_p^{(\gamma)}a_q^{(\lambda)}D_{kp} \end{pmatrix} + \\ a_p^{(\gamma)}a_i^{(\lambda)}\dfrac{\partial N_J}{\partial x_p}\left(\dfrac{1}{\Delta t}\delta_{ij} - \dfrac{\partial v_i}{\partial x_j}\right) + \\ a_p^{(\gamma)}a_i^{(\lambda)}\dfrac{\partial N_J}{\partial x_i}\left(\dfrac{1}{\Delta t}\delta_{pj} - \dfrac{\partial v_p}{\partial x_j}\right) + \end{bmatrix} \tag{31}$$

Similarly, the other Jacobean matrices are determined by

$$K_{ijIJ}^{f\theta}\Big|^{\text{int}} = \int_{\Omega^e}\left\{\begin{matrix} \dfrac{\partial N_I}{\partial x_k}\dfrac{\partial \tau_{ki}}{\partial \theta_{jJ}} + \\ \zeta\begin{pmatrix} \dfrac{\partial N_I}{\partial x_k}\dfrac{\partial \Lambda_{pj}^J}{\partial x_p} - \\ \dfrac{\partial N_I}{\partial x_p}\dfrac{\partial \Lambda_{pj}^J}{\partial x_k} \end{pmatrix}\tau_{ki} \end{matrix}\right\} d\Omega \tag{32}$$

$$K_{ijIJ}^{mu}\Big|^{\text{int}} = \int_{\Omega^e} \left\{ \begin{array}{l} \dfrac{\partial \Lambda_{qi}^{I}}{\partial x_k}\dfrac{\partial \tau_{kq}}{\partial u_{jJ}} + \\ \left(\begin{array}{l} \dfrac{\partial \Lambda_{qi}^{I}}{\partial x_k}\dfrac{\partial N_J}{\partial x_j} - \\ \dfrac{\partial \Lambda_{qi}^{I}}{\partial x_j}\dfrac{\partial N_J}{\partial x_k} \end{array} \right)\tau_{kq} \end{array} \right\} \zeta d\Omega \qquad (33)$$

$$K_{ijIJ}^{m\theta}\Big|^{\text{int}} = \int_{\Omega^e} \left\{ \begin{array}{l} \zeta \dfrac{\partial \Lambda_{qi}^{I}}{\partial x_k}\dfrac{\partial \tau_{kq}}{\partial \theta_{jJ}} + \\ \zeta^2 \left(\begin{array}{l} \dfrac{\partial \Lambda_{qi}^{I}}{\partial x_k}\dfrac{\partial \Lambda_{pj}^{J}}{\partial x_p} - \\ \dfrac{\partial \Lambda_{qi}^{I}}{\partial x_p}\dfrac{\partial \Lambda_{pi}^{J}}{\partial x_k} \end{array} \right)\tau_{kq} \end{array} \right\} d\Omega \qquad (34)$$

To obtain the kinematical Jacobean matrix, the nodal displacement derivative of Eq. (26) is taken as

$$K_{ijIJ}^{fu}\Big|^{con} = \sum_{\lambda=1}^{2} \alpha \int_{\Omega_0^e} \frac{\partial N_I}{\partial X_\delta}\frac{\partial N_J}{\partial X_\nu} \left(\begin{array}{l} F_{i\alpha}F_{j\beta} + \\ \varepsilon_{\alpha\beta}\delta_{ij} \end{array} \right) \times A_\alpha^{(\lambda)} A_\beta^{(\lambda)} A_\delta^{(\lambda)} A_\nu^{(\lambda)} d\Omega_0 \qquad (35)$$

Similarly, the other kinematical Jacobean matrices can be obtained as

$$K_{ijIJ}^{f\theta}\Big|^{con} = \sum_{\lambda=1}^{2} \alpha \int_{\Omega_0^e} \frac{\partial N_I}{\partial X_\delta}\frac{\partial \Lambda_{pj}^{J}}{\partial X_\nu} \left(\begin{array}{l} F_{i\alpha}F_{p\beta} + \\ \varepsilon_{\alpha\beta}\delta_{ip} \end{array} \right) \times A_\alpha^{(\lambda)} A_\beta^{(\lambda)} A_\delta^{(\lambda)} A_\nu^{(\lambda)} \zeta d\Omega_0 \qquad (36)$$

$$K_{ijIJ}^{mu}\Big|^{con} = \sum_{\lambda=1}^{2} \alpha \int_{\Omega_0^e} \frac{\partial \Lambda_{pi}^{I}}{\partial X_\delta}\frac{\partial N_J}{\partial X_\nu} \left(\begin{array}{l} F_{p\alpha}F_{j\beta} + \\ \varepsilon_{\alpha\beta}\delta_{pj} \end{array} \right) \times A_\alpha^{(\lambda)} A_\beta^{(\lambda)} A_\delta^{(\lambda)} A_\nu^{(\lambda)} \zeta d\Omega_0 \qquad (37)$$

$$K_{ijIJ}^{m\theta}\Big|^{con} = \sum_{\lambda=1}^{2} \alpha \int_{\Omega_0^e} \frac{\partial \Lambda_{pi}^{I}}{\partial X_\delta}\frac{\partial \Lambda_{qj}^{J}}{\partial X_\nu} \left(\begin{array}{l} F_{p\alpha}F_{q\beta} + \\ \varepsilon_{\alpha\beta}\delta_{pq} \end{array} \right) \times A_\alpha^{(\lambda)} A_\beta^{(\lambda)} A_\delta^{(\lambda)} A_\nu^{(\lambda)} \zeta^2 d\Omega_0 \qquad (38)$$

The finite element Eq. (28) is used to calculate deformation field by modifying the initial assumed displacement and rotation of transverse planes in order to reduce the nodal residual force and force values to an acceptable tolerance.

5 Computational Method

To analyze the forming process of reinforced thermoplastic ply, the total process is divided into a convenient number of increments and the calculated deformed configuration for a single time step is used as input for the next time step. To calculate the nodal displacement at mid-surface and the rotation of transverse plane at the end of each increment, a computer program has been developed based on the finite element formulation. In the first iteration, the input deformed configuration is assumed to be the material geometry at the end of increment in order to calculate the current fiber directions and ply thickness at the end of increment. This assumption will be modified as the iterative procedure proceeds. The mid-surface geometry is also used to construct the corotational coordinate system at each integration point using the method developed by Hughes [11]. Using the current fiber directions and ply thickness to calculate Jacobean matrices, the increment of displacement and transverse plane rotation can be computed. After modification of the assumed material position at the end of increment, it is used to calculate the fiber directions and ply thickness. The procedure is repeated until the convergence criteria are satisfied.

Convergence of iterative solution method is evaluated by ensuring that all components of nodal residual forces/moments and nodal displacement/rotation corrections are sufficiently small. As described in section (4.2), the nodal residual forces and moments are used to modify the displacement increment in Newton-Raphson iterative solution method. The solution of nonlinear equation is accepted when the absolute value of maximum residual force/moment is less than a tolerance value that is set to 0.5% of average nodal force/moment in

the computer program. To terminate iterations, the displacement and rotation correction values at all nodes must also be less than a fraction (1%) of total incremental displacement and rotation vectors, respectively.

6 Results and Discussions

The presented finite element procedure is used to simulate the hemisphere forming process of thermoplastic ply reinforced with woven fabric. In this process, a hemisphere punch moves the pre-heated lamina into the die cavity while the friction force in blank holder region restricts the material flow. Since the tools have enough rigidity compared to heated composite ply, the tool surfaces are mesh using the analytical rigid elements. Fig. (2) shows the mesh configuration in the composite lamina and tool surfaces in which one quarter of geometry is considered and the symmetry conditions are applied where necessary. An exponential function is used to model the normal contact force in order to improve the convergence rate in the solution method. The radius of hemispherical punch and die cavity is 27 mm and 30 mm, respectively, in which a gap of 3 mm ensures the ease of lamina flow into the die cavity. The fillet radius of all tool corners is 5 mm. The composite blank has the dimensions of 150 mm×150 mm and its initial thickness is 1 mm. The laminate is meshed using shell elements with eight nodes and six degree-of-freedom on each node. In the initial geometry the woven fibers are parallel to the sides of the square blank.

Fig. (3) shows the calculated deformed geometry after the punch has moved the blank into the die cavity to the depth of 27 mm with forming speed of 27 mm/s. Due to high anisotropic behavior of reinforced ply, the amount of radial displacement varies considerably on the outer side. There is a significant radial displacement along the fiber directions because the fiber inextensibility constrain. It enforces the deformation at the center of blank to propagate to the outer edges. Due to the trellis-like shear deformation in which yarn families rotate at the crossover points, there is considerable stretch along the lines at angle of ±45° respect to initial fiber directions. Therefore, the punch penetration at the blank center causes little radial flow along these lines.

Fig. (3) also shows the calculated angle between the fiber families in which the initially perpendicular fibers have considerable angle reduction along the lines at angle of ±45° and at the region A. The severe shear deformation is the effective reason of the angle change at this

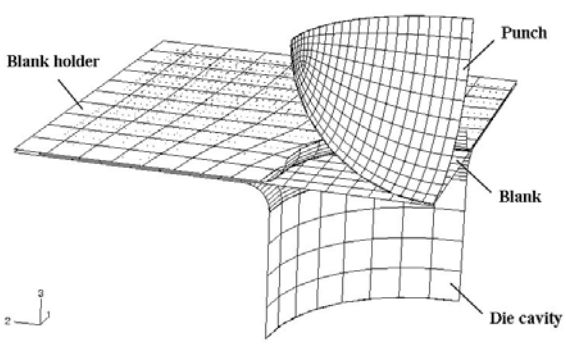

Fig.2. One quarter of the mesh geometry of composite blank and hemispherical stamp forming tool

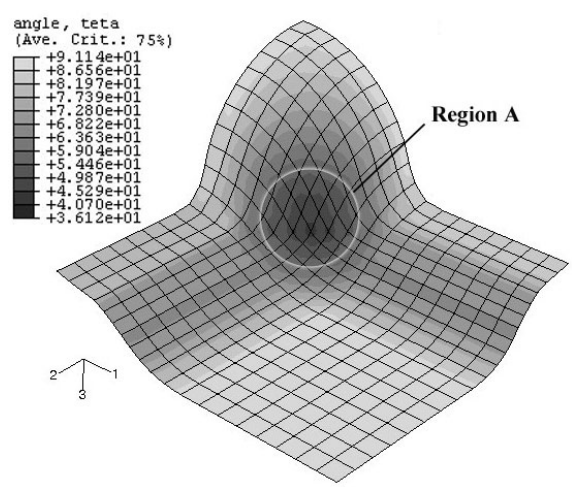

Fig. 3. The calculated deformed geometry and angle between woven fibers in the hemispherical stamp forming process

region. The analysis of woven fabric showed [13] that the angle reduction is possible up to a critical value and for more values, the fiber deformation locks and wrinkling takes place. Thus, the calculated angle between fibers is an important numerical results obtained by the presented finite element method and it provides convenient criteria to estimate the presence of the wrinkling defects in the final geometry of woven reinforced thermoplastic plies.

7 Conclusions

The presented finite element formulation provides an appropriate procedure to model the forming process of thermoplastic layer reinforced with continuous fibers. Using Mindlin-Reissner assumptions in the shell formulation and anisotropic viscous model for reinforced thermoplastic materials at the forming temperature, the deformed geometry is computed considering the predominated deformation mechanisms and the rate of deformation effect. Unlike the quasi-static method that the nodal deformation may deviate from the kinematical constrains and tool contact boundary conditions, the solution method converges when the calculated deformed geometry satisfies the kinematical constrains and boundary conditions. The presented shell finite element method can be extended to numerical large deformation analysis of materials that their behavior depends on the rate of deformation.

References

[1] Abadi M. T., Daghyani H. R. , Fariborz S.., “Experimental Wrinkling Analysis in Stamp Forming of Continuous Fiber Reinforced Thermoplastic Sheets”, *Proceedings of International Congress in Manufacturing Engineering*, Tehran, Iran, 2005.

[2] Advani S. G., Creasy T. S. and Shuler S. F., “Rheoelogy of Long Fiber- Reinforced Composites in Sheet Forming”, in: Bhattacharyya D., editor, *Composite sheet forming*, Composite material series, Vol. 11, Elsevier Pub. , 1997.

[3] Spencer A. J. M., “Theory of Fabric-Reinforced Viscose Fluid”, *Composite Part A*, Vol. 31, pp. 1311-1321, 2000.

[4] Ó Brádaigh C. M. and Pipes R. B., “Finite Element Analysis of Composite Sheet-Forming Processes”, *Composites Manufacturing*, Vol. 2, Nos. 3 & 4, pp. 164-170, 1991.

[5] Ó Brádaigh C. M., McGuinness G. B., McEntee S.P., “Implicit Finite Element Modelling of Composites Sheet Forming Processes”, in: Bhattacharyya D., editor, *Composite sheet forming*, Composite material series, Vol. 11, Elsevier Pub. , 1997.

[6] McEntee S. P. and Ó Brádaigh C. M., “Large Deformation Finite Element Modeling of Single-Curvature Composite Sheet Forming With Tool Contact”, *Composites Manufacturing*, Vol. 6, 269-280, 1998.

[7] Johnson A. F., Pickett A. K., “Numerical Simulation of the Forming Process in Long Fiber Reinforced Thermoplastic”, *CADCOMP ’96*, Udine, Italy, 1996.

[8] Abadi M. T., "Thermoforming process analysis of woven fabric reinforced thermoplastic composites", *Proceedings of the Eighth International Conference on Computational Structures Technology*, B.H.V. Topping, G. Montero and R. Montenegro, (Editors), Civil-Comp Press, Stirlingshire, United Kingdom, paper 91, 2006.

[9] Yu W. R., Zampaloni M., Pourboghrat F., Chung K. and Kang T. J., "Sheet hydroforming of Woven FRT Composites: Non-Orthogonal Constitutive Equation Considering Shear Stiffness and Undulation of Woven Structure", *Composite Structures*, Vol. 61, pp. 353-362, 2003.

[10] Cao J., Xue P., Peng X. and Krishnan N., "An Approach in Modelling the Temperature Effect in Thermo-stamping of Woven Composites", *Composite Structures*, Vol. 61, 2003, pp. 413-420.

[11] McGuinness G. B., Ó Brádaigh C. M., "Development of Rheological Models for Forming Flows and Picture-Frame Shear Testing of Fabric Reinforced Thermoplastic Sheets", *Journal of Non-Newtonian Fluid Mechanics*, Vol. 73, 1-28, 1997.

[12] Hughes T. J. R., *"The Finite Element Method, Linear Static and Dynamic Finite Element Analysis",* Prentice-Hall, Englewood Cliffs, NJ, 1987.

[13] King M. J, Jearanaisilawong P. and Socrate S., "A Continuum Constitutive Model for the Mechanical Behavior of Woven Fabrics", *International Journal of Solids and Structures*, Vol. 42, No. 13, pp. 3867-3896, 2005.